J. Fluid Mech. (2018), *vol.* 851, R1, doi:10.1017/jfm.2018.506

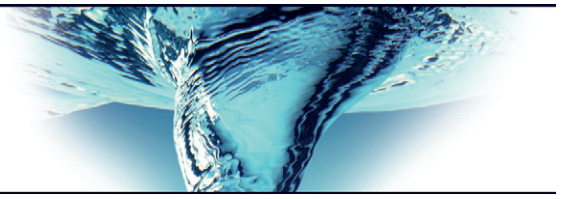

JFM RAPIDS
journals.cambridge.org/rapids

Streamwise self-similarity and log scaling in turbulent boundary layers

Shivsai Ajit Dixit[1],† **and O. N. Ramesh**[2]

[1]Indian Institute of Tropical Meteorology, Pashan, Pune-411008, India

[2]Department of Aerospace Engineering, Indian Institute of Science, Bengaluru-560012, India

(Received 1 February 2018; revised 20 April 2018; accepted 18 June 2018;
first published online 19 July 2018)

High Reynolds number is thought to be a fundamental condition essential for the occurrence of log scaling in turbulent boundary layers. However, while log variation of mean velocity is seen to occur at moderate Reynolds numbers in the traditional boundary layer literature, log variations of higher-order moments are evident only at much higher Reynolds numbers, as reported in recent experiments. This observation suggests that, underlying the occurrence of log scaling in turbulent boundary layers, there exists a more fundamental condition (apart from the largeness of Reynolds number) – the requirement of self-similar evolution of a mean-flow quantity of interest along a mean-flow streamline, i.e. the mean advection of the scaled mean quantity of interest is required to be zero. Experimental data from the literature provide strong support for this proposal.

Key words: turbulent boundary layers, turbulent flows

1. Introduction

The log scaling for the mean velocity in turbulent boundary layers (TBLs) has been extensively studied in the literature. Recently, data from high-Reynolds-number (high-*Re*) high-quality laboratory experiments have become available and have convincingly shown that the region of log variation at high Reynolds numbers is quite comprehensive, i.e. not only the mean velocity but also the variance (Marusic *et al.* 2013; Vallikivi, Hultmark & Smits 2015) and higher-order even moments of velocity fluctuation in the x direction (x is the wall-parallel coordinate along the flow) show log variations over an overlapping range of wall-normal locations (Meneveau & Marusic 2013; Vallikivi *et al.* 2015). With further analysis of these data sets, we find that beyond δ_+ of approximately 7000, the variances of velocity fluctuations in the spanwise (z) and wall-normal (y) directions and the Reynolds shear stress also follow

† Email address for correspondence: sadixit@tropmet.res.in

log variations over the same range of wall-normal locations (see figure 1*a*). When data for the third-order moment (reconstructed from the skewness factor profiles) from the experiments of Marusic *et al.* and Vallikivi *et al.* are analysed, we find that this (odd) moment also follows log variation which, however, occurs at a much higher Reynolds number ($\delta_+ \geqslant 70\,000$) in comparison with the log scaling of even moments (see figure 1*b*). Two questions therefore arise from these observations. (1) Why is the log variation of the mean velocity in the inertial sublayer (ISL) evident even at moderate Reynolds numbers whereas log variations of higher-order moments show up only at much higher Reynolds numbers? (2) Why do log variations of odd moments occur at much higher Reynolds numbers compared with those of even moments? Towards answering these questions, we show that in TBL flows, the self-similarity of a mean-flow quantity along a mean streamline (henceforth, streamwise self-similarity) in the ISL results in the log variation of that quantity; this is equivalent to zero advection of the quantity, scaled appropriately by the friction velocity u_τ. Conversely, we also show that the existence of log scaling of a scaled mean-flow quantity leads to the zero-advection condition or streamwise self-similarity. Streamwise self-similarity in the present context should not be confused with the more common notion of self-similarity in the x direction (e.g. as in laminar boundary layers). This distinction is crucial – it can be easily shown that Falkner–Skan solutions of laminar boundary layers, while being self-similar in x, are not streamwise self-similar in general, i.e. the mean advection in Falkner–Skan flows is not always zero (e.g. Blasius boundary layer).

The present paper is organized as follows. Section 2 presents theoretical analysis of the zero-advection condition and its relation to the occurrence of log scaling. In the context of the present proposal, § 3 examines experimental data from the literature on canonical zero-pressure-gradient (ZPG) TBL flows over a wide range of Reynolds numbers. Section 4 summarizes the conclusions.

2. Zero-advection condition and log scaling in TBL flows

In a seminal work, Coles (1955) proposed the so-called streamline hypothesis for TBLs according to which a necessary and sufficient condition for a universal law of the wall for the mean velocity in the inner region is that the ratio $\langle u/u_\tau \rangle$ be constant on streamlines of the mean flow (i.e. streamwise self-similarity). This implies that the iso-y_+ lines would be identical to the mean streamlines in the inner region. Coles averred that 'this result must surely be considered in any search for a fundamental order and unity in the description of turbulent shear flows' (Coles 1956). In the present work, we build on this description to obtain a generalized streamline hypothesis (streamwise self-similarity or zero advection) for higher-order moments of fluctuating velocity. In particular, we shall consider advection of a scaled mean quantity Q_+ in a steady two-dimensional TBL flow,

$$\mathrm{ADV}(Q_+) \triangleq \langle \boldsymbol{u} \rangle \cdot \boldsymbol{\nabla} Q_+ = \langle u \rangle \frac{\partial Q_+}{\partial x} + \langle v \rangle \frac{\partial Q_+}{\partial y}. \tag{2.1}$$

Here, $\langle u \rangle$ and $\langle v \rangle$ are the components of the mean velocity vector $\langle \boldsymbol{u} \rangle$ in the x and y directions respectively. It should be noted that $\langle \boldsymbol{u} \rangle \cdot \boldsymbol{\nabla} Q_+$ – dimensional advection of non-dimensional Q_+ – represents the spatial rate of change of Q_+ along a mean-flow streamline; Q_+ could be the normalized mean velocity $\langle u_+ \rangle$ or generalized mixed moments $\langle u_+'^m v_+'^n \rangle^{2/(m+n)}$ of velocity fluctuations in the x and y directions; mixed

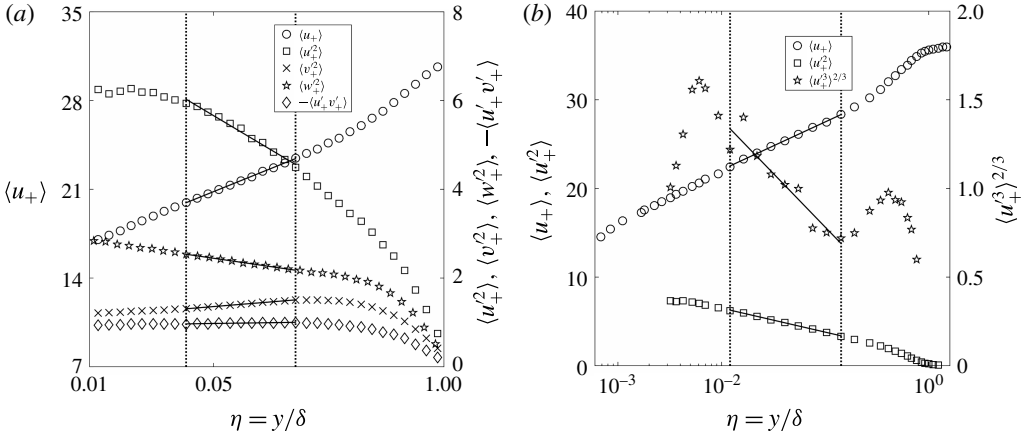

FIGURE 1. Log scaling in high-Re TBL flows from the literature. Profiles of (a) mean velocity $\langle u_+\rangle$, variance $\langle u_+'^2\rangle$ in the x direction, wall-normal (y direction) variance $\langle v_+'^2\rangle$, spanwise (z direction) variance $\langle w_+'^2\rangle$ and Reynolds shear stress $-\langle u_+'v_+'\rangle$ at $\delta_+ = 10\,768$ (case TBHM1 of table 1; see Talluru *et al.* 2014), and (b) $\langle u_+\rangle$, $\langle u_+'^2\rangle$ and third-order moment $\langle u_+'^3\rangle^{2/3}$ at $\delta_+ = 72526$ (case VHS7 of table 1; see Vallikivi *et al.* 2015). The third moment data are reconstructed from figures 4(a) and 9(a) of Vallikivi *et al.* The wall-normal distance is expressed in outer coordinates $\eta = y/\delta$, and $u_\tau = \sqrt{\tau_w/\rho}$ is the friction velocity, τ_w is the wall-shear stress, ρ and ν are respectively the density and kinematic viscosity of the fluid, and the boundary layer thickness $\delta = \delta_{99}$ is defined as the wall-normal distance where $\langle u\rangle$ becomes 99 % of the free-stream velocity u_∞ (see table 1). The subscript $+$ denotes non-dimensionalization using u_τ for velocities and u_τ and ν for distances, and $\langle\ \rangle$ indicates time averaging. The solid lines show least-squares log fits to data over the comprehensive log region, shown by vertical dotted lines, with the extent $y_+ \geqslant 3.6\sqrt{\delta_+}$ to $\eta \leqslant 0.12$, i.e. approximately 35 % of a decade, in (a) and $y_+ \geqslant 3\sqrt{\delta_+}$ to $\eta \leqslant 0.14$, i.e. 125 % of a decade, in (b).

moments may be considered as generalizations of the even moments of u_+' studied in the literature (Meneveau & Marusic 2013).

In the inner region (including the ISL), the law-of-the-wall scaling for the mean velocity in the x direction,

$$\langle u\rangle = u_\tau f(y_+), \tag{2.2}$$

along with the continuity equation, $\partial\langle u\rangle/\partial x + \partial\langle v\rangle/\partial y = 0$, leads to

$$\langle v\rangle = -yf\frac{\mathrm{d}u_\tau}{\mathrm{d}x}. \tag{2.3}$$

Assuming that the law of the wall for the mean velocity holds, i.e. (2.2) and (2.3) are valid, we proceed in the following sections to show that

(i) the zero-advection requirement of Q_+ follows from its log variation with y (or y_+) and conversely
(ii) the log variation of Q_+ with y (or y_+) follows from its zero-advection requirement.

https://doi.org/10.1017/jfm.2018.506 Published online by Cambridge University Press

Flow Code	δ_+	δ (m)	u_∞ (m s^{-1})	u_τ (m s^{-1})	ν/u_τ (μm)	S	C_f	$\delta(\mathrm{d}S/\mathrm{d}x)$	x (m)	$\mathrm{d}u_\tau/\mathrm{d}x$ (s^{-1})	x_s (m)	$x/u_\tau(\mathrm{d}u_\tau/\mathrm{d}x)$	R_δ	θ/δ	$\mathrm{d}\delta_+/\mathrm{d}x_+$
Princeton moderate-/high-Re ZPG TBLs															
VHS1	2 622	0.0262	9.08	0.3296	10.0	27.5484	0.00264	0.02828	1.789	−0.012906	25.538	−0.070047	72 232	0.1128	0.01131
VHS2	4 635	0.0273	9.21	0.3166	5.9	29.0860	0.00236	0.02643	2.111	−0.010522	30.094	−0.070153	134 814	0.1111	0.01057
VHS3	8 261	0.0281	9.29	0.3034	3.4	30.6237	0.00213	0.02480	2.487	−0.008747	34.681	−0.071698	252 982	0.1090	0.00992
VHS4	14 717	0.0265	9.33	0.2915	1.8	32.0108	0.00195	0.02349	2.420	−0.008075	36.096	−0.067057	471 102	0.0968	0.00940
VHS5	25 062	0.0251	9.46	0.2836	1.0	33.3548	0.00180	0.02235	2.358	−0.007582	37.404	−0.063030	835 938	0.0963	0.00894
VHS6	40 053	0.0240	9.50	0.2751	0.6	34.5269	0.00168	0.02144	2.319	−0.007109	38.706	−0.059920	1 382 906	0.0983	0.00857
VHS7	72 526	0.0290	9.55	0.2661	0.4	35.8925	0.00155	0.02046	2.891	−0.005229	50.883	−0.056820	2 603 139	0.0872	0.00819
Melbourne moderate-/high-Re ZPG TBLs															
HMMM1	2 568	0.0853	12.50	0.4575	33.2	27.3197	0.00268	0.02858	5.784	−0.005613	81.510	−0.070967	70 160	0.1160	0.01143
MCKH1	3 914	0.0838	20.24	0.7068	21.4	28.6359	0.00244	0.02695	6.235	−0.007940	89.015	−0.070039	112 068	0.1144	0.01078
MCKH2	6 575	0.1473	20.50	0.6824	22.4	30.0376	0.00222	0.02540	12.262	−0.003918	174.155	−0.070408	197 508	0.1109	0.01016
MCKH3	7 925	0.1833	19.97	0.6607	23.1	30.2228	0.00219	0.02521	16.184	−0.003006	219.798	−0.073632	239 529	0.1083	0.01008
MCKH4	10 529	0.2507	19.91	0.6391	23.8	31.1582	0.00206	0.02428	22.487	−0.001987	321.679	−0.069904	328 072	0.1070	0.00971
TBHM1	10 768	0.2677	19.00	0.6073	24.9	31.2881	0.00204	0.02416	24.051	−0.001751	346.784	−0.069354	336 898	0.1079	0.00966
Stanford low-/moderate-Re ZPG TBLs															
DE1	1 084	0.0414	9.84	0.4030	38.2	24.4113	0.00336	0.03299	2.315	−0.013153	30.640	−0.075555	26 457	0.1131	0.01319
DE2	1 700	0.0360	18.95	0.7270	21.2	26.0656	0.00294	0.03033	2.233	−0.023468	30.979	−0.072067	44 321	0.1167	0.01213
DE3	4 295	0.0342	14.31	0.5120	8.0	27.9434	0.00256	0.02778	2.583	−0.014871	34.430	−0.075015	120 026	0.1063	0.01111

TABLE 1. Various parameters for the Princeton (Vallikivi *et al.* 2015, flow code VHS), Melbourne (Harun *et al.* 2013; Talluru *et al.* 2014; Marusic *et al.* 2015, flow codes HMMM, TBHM and MCKH respectively) and Stanford (DeGraaff & Eaton 2000, flow code DE) ZPG TBL data sets. It should be noted that the Melbourne data have $Re_\tau = \delta_c u_\tau/\nu = 3020$, 4945, 8280, 10 489, 13 386 and 15 000 respectively, where δ_c is a measure of the boundary layer thickness different from $\delta = \delta_{99}$; $\delta_c > \delta$ (Jones, Marusic & Perry 2001; Monkewitz, Chauhan & Nagib 2008). We have used $\delta_+ = \delta u_\tau/\nu = \delta_{99} u_\tau/\nu$, where δ has been obtained from the mean velocity profile. Original data sets have been used for the analysis of the Melbourne experiments, whereas mean velocity profiles have been digitized from Vallikivi *et al.* (2015) and DeGraaff & Eaton (2000) for the analysis of the Princeton and Stanford experiments respectively. Here, $x_s = -u_\tau/(\mathrm{d}u_\tau/\mathrm{d}x)$ is the distance of the virtual wall source upstream of the measurement location according to the kinematic description of Coles (1955); see figure 2 of § 2.2.

2.1. *Zero advection of Q_+ follows from its log variation with y*

For $Q_+ = \langle u_+ \rangle$, (2.2) gives $\partial\langle u_+\rangle/\partial x = [y(\mathrm{d}u_\tau/\mathrm{d}x)/\nu]\mathrm{d}f/\mathrm{d}y_+$ and $\partial\langle u_+\rangle/\partial y = (u_\tau/\nu)\mathrm{d}f/\mathrm{d}y_+$. Substitution of these expressions along with (2.2) and (2.3) in (2.1) yields

$$\mathrm{ADV}(\langle u_+\rangle) = \langle u\rangle \frac{\partial\langle u_+\rangle}{\partial x} + \langle v\rangle \frac{\partial\langle u_+\rangle}{\partial y} = 0 \tag{2.4}$$

in the entire inner region (including the ISL, i.e. the log scaling region) for arbitrary values of δ_+. This is consistent with the experimental observation of log variation for mean velocity occurring even at moderate Reynolds numbers (δ_+ of order 10^3; see, for example, Fernholz & Finley 1996; DeGraaff & Eaton 2000). The slope of a mean streamline in the inner region is $\mathrm{d}y/\mathrm{d}x = \langle v\rangle/\langle u\rangle = -y(\mathrm{d}u_\tau/\mathrm{d}x)/u_\tau$ and is equal to the slope of an iso-y_+ line there; the latter may be obtained from the condition $\mathrm{d}(yu_\tau) = 0$. Thus, mean streamlines and iso-y_+ lines coincide in the inner region (including the ISL), and there is no mean exchange ('entrainment') of fluid between the outer wake region and the inner region. This, in essence, is Coles' streamline hypothesis for mean velocity (Coles 1955).

Now, we generalize this to higher-order moments of velocity fluctuations, such as variance. Velocity fluctuations in the near-wall region are known to be influenced by outer-scaled motions through the so-called amplitude modulation effects. Hence, in this region, velocity fluctuation in the x direction can be expressed (Marusic, Mathis & Hutchins 2010*a*) as

$$u'_+(y_+, \eta, t) = g_{1,u}(y_+, t)g_{2,u}(\eta, t) + g_{3,u}(\eta, t), \tag{2.5}$$

where t is the time coordinate, $y_+ = yu_\tau/\nu$ ($\eta = y/\delta$) is the wall-normal distance in inner (outer) coordinates, $g_{1,u}$ is the statistically universal near-wall component and $g_{2,u}$ and $g_{3,u}$ are respectively the amplitude modulation and linear superposition effects of outer-scaled motions (Marusic *et al.* 2010*a*). Since the wall-normal velocity fluctuation v' is also modulated in a similar fashion to u' (Talluru *et al.* 2014), an expression for v'_+ may be written similarly to that for u'_+ given above. For a generalized mixed moment $Q_+ = \langle u'^m_+ v'^n_+\rangle^{2/(m+n)}$ in the inner region, these expressions lead to the functional form $Q_+ = Q_+(y_+, \eta)$ or $Q_+(y_+, \delta_+)$, where, in general, the variables are not separable. Indeed, experiments show that the log variations of variance of u'_+ at different Reynolds numbers in a TBL do not collapse in inner as well as outer scaling but exhibit a systematic shift with δ_+ (see figures 4*a*, 6*a* and 6*c* in Vallikivi *et al.* 2015). Substitution of $Q_+ = Q_+(y_+, \delta_+)$ in the definition of $\mathrm{ADV}(Q_+)$ yields

$$\mathrm{ADV}(Q_+) = \mathrm{ADV}(\langle u'^m_+ v'^n_+\rangle^{2/(m+n)}) = u_\tau f \frac{\mathrm{d}\delta_+}{\mathrm{d}x}\frac{\partial Q_+}{\partial \delta_+}, \tag{2.6}$$

which could become zero when

$$\frac{\mathrm{d}\delta_+}{\mathrm{d}x} \to 0. \tag{2.7}$$

This shows that even a complicated functional form such as $Q_+(y_+, \delta_+)$ can result in $\mathrm{ADV}(Q_+) = 0$ provided that the condition $\mathrm{d}\delta_+/\mathrm{d}x \to 0$ is satisfied; the role of $\partial Q_+/\partial\delta_+$ towards explaining experimental observations of even and odd moments will be discussed in § 4. Physically, the condition $\mathrm{d}\delta_+/\mathrm{d}x \to 0$ implies that the mean

streamlines of the flow in the inner region (including the ISL) of a TBL flow tend to be straight lines ($\mathrm{d}y/\mathrm{d}x = \langle v\rangle/\langle u\rangle = \text{const.}$ along a mean streamline) and concomitantly become orientated parallel to the wall (the slope $\mathrm{d}y/\mathrm{d}x \to 0$, see figure 4*b*). Thus, the condition $\mathrm{d}\delta_+/\mathrm{d}x \to 0$ effectively reduces to $[\langle v_A\rangle/\langle u_A\rangle = \langle v_B\rangle/\langle u_B\rangle]_{y_+}$, where $\langle u\rangle$ and $\langle v\rangle$ are measured at the same value of y_+ in the inner layer (i.e. on the same mean streamline) but at different measurement stations A and B along the x direction.

In order to see that the condition $\mathrm{d}\delta_+/\mathrm{d}x \to 0$ is closely approximated in canonical ZPG TBLs only at high Reynolds numbers, we consider the so-called skin-friction law

$$S = \kappa^{-1}\ln(\delta_+) + D, \tag{2.8}$$

where $S = u_\infty/u_\tau$ and D is a constant. Differentiation of both sides with respect to x and rearrangement yield

$$\frac{\mathrm{d}\delta_+}{\mathrm{d}x} = \kappa\frac{u_\infty}{\nu}\left(\frac{\delta}{S}\frac{\mathrm{d}S}{\mathrm{d}x}\right), \tag{2.9}$$

where κ, u_∞ and ν are constants in a given ZPG TBL flow developing in the x direction. Jones, Nickels & Marusic (2008) have shown that $\delta/S(\mathrm{d}S/\mathrm{d}x) \to 0$ as $\delta_+ \to \infty$ in ZPG TBL flows, implying that $\mathrm{d}\delta_+/\mathrm{d}x \to 0$ in the limit of infinite Reynolds number. Section 3 presents evaluation of different ZPG TBL experiments in the literature with respect to the zero-advection condition.

As an interim summary, so far we have shown that in the ISL of a TBL flow, (i) the functional form of the dimensionless mean velocity satisfies the corresponding zero-advection condition (Coles 1955) for even moderate values of the Reynolds number δ_+, (ii) the functional form of the dimensionless generalized mixed moments satisfies the corresponding zero-advection condition when $\mathrm{d}\delta_+/\mathrm{d}x \to 0$, and this is satisfied only at high Reynolds numbers in canonical ZPG TBLs.

2.2. *Log variation of Q_+ with y follows from its zero advection*

Starting from the premise $\mathrm{ADV}(Q_+) = 0$, one obtains

$$\frac{\partial Q_+}{\partial y} = -\frac{\langle u\rangle}{\langle v\rangle}\frac{\partial Q_+}{\partial x}, \tag{2.10}$$

where the ratio $\langle u\rangle/\langle v\rangle$, from (2.2) and (2.3), at any y in the inner region is

$$\frac{\langle u\rangle}{\langle v\rangle} = -\frac{u_\tau/(\mathrm{d}u_\tau/\mathrm{d}x)}{y} = \frac{x_s}{y_s}. \tag{2.11}$$

Here, $x_s = -u_\tau/(\mathrm{d}u_\tau/\mathrm{d}x)$ and $y_s = y$ are length scales in the x and y directions respectively; $y_s = y$ is predicated on the existence of an ISL (Tennekes & Lumley 1972). If $\partial Q_+/\partial x$ is independent of y, as we shall confirm *a posteriori*, then (2.10) and (2.11) immediately lead to log scaling of Q_+.

Before proceeding further, it is instructive to consider a kinematic interpretation of the streamwise length scale x_s. According to Coles (1955), x_s geometrically represents the distance, upstream of a streamwise measurement station, of the common point of intersection (located on the solid wall) of all mean velocity vectors in the inner region at that station (see figure 2). These vectors can be imagined to be emanating from a virtual source point on the wall located a distance x_s upstream. Coles (1955) showed that the kinematic picture depicted in figure 2 immediately follows from the law of the wall for the mean velocity. In a ZPG TBL, x_s increases with the Reynolds

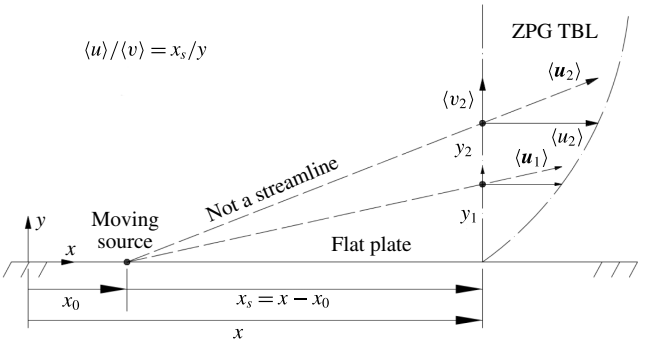

FIGURE 2. Geometrical interpretation of the streamwise length scale x_s in the inner layer of a ZPG TBL following Coles (1955). The dashed lines represent the directions of the mean velocity vectors $\langle \boldsymbol{u}_1\rangle$ and $\langle \boldsymbol{u}_2\rangle$ at two representative heights y_1 and y_2 in the inner layer. The dashed–dotted line indicates the mean velocity profile.

number δ_+ (see table 1), i.e. the virtual source point moves further upstream of the measurement location. Therefore, mean streamlines in the inner region (including the ISL) would tend to straight lines emanating from the virtual source (dashed lines in figure 2) and would be nearly parallel to the wall (see figure 4*b*) at high Reynolds numbers as $\mathrm{d}\delta_+/\mathrm{d}x \to 0$.

Next, one may write the asymptotic expansion (Van Dyke 1975) for Q_+ in the ISL as

$$Q_+(y_+;\, \delta_+) = \epsilon_0(\delta_+)h_0(y_+) + \epsilon_1(\delta_+)h_1(y_+) + \cdots, \tag{2.12}$$

where $\epsilon_0, \epsilon_1, \ldots$ are gauge functions (capturing δ_+ dependence of Q_+, if any) in decreasing order such that $Q_+/\epsilon_0 h_0 \to 1$ and $\epsilon_1/\epsilon_0 \to 0$ as $\delta_+ \to \infty$, and $h_0, h_1, \ldots$ are coefficients (capturing y_+ dependence of Q_+), where h_0 is a constant of $O(1)$. It should be noted that for mean velocity $Q_+ = \langle u_+\rangle$, $\epsilon_0, \epsilon_1, \ldots$ are constants in view of the law of the wall (2.2). For ZPG TBLs, the lower end of the log region occurs at $y_{+,1} = y_1 u_\tau/\nu \approx 3\sqrt{\delta_+}$ and the upper end is located at $\eta_2 = y_2/\delta = 0.15$, i.e. $y_{+,2} = 0.15\delta_+$ (Marusic *et al.* 2013). The mean velocity profile in the log region is given by $\langle u_+\rangle = \kappa^{-1}\ln(y_+) + B$, where κ^{-1} is the slope in the semi-logarithmic inner co-ordinates and B is the intercept. The maximum slope of the mean velocity profile in the log region occurs at $y_{+,1}$, and in the limit of $\delta_+ \to \infty$ it is given by

$$\lim_{\delta_+\to\infty} \left.\frac{\mathrm{d}\langle u_+\rangle}{\mathrm{d}y_+}\right|_{y_{+,1}} = \frac{1}{\kappa y_{+,1}} = \lim_{\delta_+\to\infty} \frac{1}{3\kappa\sqrt{\delta_+}} \to 0. \tag{2.13}$$

Therefore, $\langle u_+\rangle = \epsilon_0 h_0$ is the lowest-order approximation for $\langle u_+\rangle$ in the ISL and is independent of y_+ as well as δ_+. For variance of u'_+, i.e. $Q_+ = \langle u'^2_+\rangle$, a recent work (Monkewitz & Nagib 2015) suggests that $\langle u'^2_+\rangle$ in the inner region is likely to be bounded and tends to a constant value (independent of y_+) as $\delta_+ \to \infty$. Therefore, to the lowest order, $\langle u'^2_+\rangle = \epsilon_0 h_0$ in the ISL. Extending this to the generalized moments $\langle u'^m_+ v'^n_+\rangle^{2/(m+n)}$, one may expect them to remain bounded and tend to their respective constant values as $\delta_+ \to \infty$; it should be noted that h_0 and ϵ_0 will, in general, be different for different moments. With this, $\partial Q_+/\partial x \sim \epsilon_0 h_0/x_s$ to the lowest order in the ISL and (2.10) and (2.11) yield

$$\frac{\partial Q_+}{\partial y} \sim \frac{x_s}{y_s}\frac{\epsilon_0 h_0}{x_s} \sim \frac{\epsilon_0 h_0}{y}. \tag{2.14}$$

Integration of (2.14) yields $Q_+ \sim \ln(y)$, which may be written in inner and outer coordinates respectively as

$$Q_+ = A_{m,n} \ln(y_+) + B_{m,n}, \tag{2.15}$$

$$Q_+ = A_{m,n} \ln(\eta) + C_{m,n}. \tag{2.16}$$

Here, $A_{m,n}$, $B_{m,n}$ and $C_{m,n}$ are coefficients that, in general, depend on the Reynolds number δ_+. For the mean velocity, $A_{m,n}$ is κ^{-1} and is a constant for TBLs (Marusic *et al.* 2010*b*). Lastly, we may now check *a posteriori* whether $\partial Q_+/\partial x$ is indeed independent of y. Towards this, we write $\partial Q_+/\partial x = \partial Q_+/\partial y_+[y(\mathrm{d}u_\tau/\mathrm{d}x)/\nu] + \partial Q_+/\partial \delta_+[\mathrm{d}\delta_+/\mathrm{d}x]$. For the mean velocity, the second term is identically zero since $\partial Q_+/\partial \delta_+ = 0$ due to (2.2); for generalized mixed moments, this term tends to zero at high Reynolds numbers due to $\mathrm{d}\delta_+/\mathrm{d}x \to 0$. Use of (2.15) in the first term leads to $\partial Q_+/\partial x = -A_{m,n}/x_s$, which is independent of y.

To summarize, for TBL flows, if one starts with the assertion of zero advection of Q_+ in the ISL, log variation of Q_+ follows, and vice versa.

3. Appraisal of experimental data from canonical ZPG TBLs

The physical basis for the analysis presented in § 2 is invariance of a generalized scaled mean-flow quantity Q_+ along a mean streamline in a given flow. This leads to the consideration of dimensional advection $\mathrm{ADV}(Q_+)$ being zero. However, in order to compare the zero-advection conditions in different ZPG TBLs, a dimensionless framework is required.

We consider dimensional and dimensionless advection operators $\mathrm{ADV} = u\partial/\partial x + v\partial/\partial y$ and $\mathrm{ADV}_+ = u_+\partial/\partial x_+ + v_+\partial/\partial y_+$ respectively. Here, $u_+ = u/u_\tau$, $v_+ = v/u_\tau$, $x_+ = xu_\tau/\nu$ and $y_+ = yu_\tau/\nu$; x is the distance from a suitable virtual origin measured along the wall in the flow direction. For $x/u_\tau(\mathrm{d}u_\tau/\mathrm{d}x) \ll 1$, these operators are related as

$$\mathrm{ADV} = \left(\frac{u_\tau^2}{\nu}\right) \mathrm{ADV}_+, \tag{3.1}$$

and $\mathrm{ADV}(Q_+) = 0$ is equivalent to $\mathrm{ADV}_+(Q_+) = 0$. Using (3.1) in (2.6), one obtains

$$\mathrm{ADV}_+(Q_+) = f\frac{\mathrm{d}\delta_+}{\mathrm{d}x_+}\frac{\partial Q_+}{\partial \delta_+}, \tag{3.2}$$

which tends to zero if $\mathrm{d}\delta_+/\mathrm{d}x_+ \to 0$. Using (2.9), one obtains

$$\frac{\mathrm{d}\delta_+}{\mathrm{d}x_+} = \kappa\left(\delta\frac{\mathrm{d}S}{\mathrm{d}x}\right). \tag{3.3}$$

Jones *et al.* (2008) have shown that $\delta(\mathrm{d}S/\mathrm{d}x) \to 0$ as $\delta_+ \to \infty$ in ZPG TBLs, implying that $\mathrm{d}\delta_+/\mathrm{d}x_+ \to 0$ as well in the limit of infinite Reynolds number.

We now consider mean velocity data from Princeton, Melbourne and Stanford experiments covering a wide range of Reynolds numbers $1000 < \delta_+ < 73\,000$ (see table 1) and initially focus on the requirement $x/u_\tau(\mathrm{d}u_\tau/\mathrm{d}x) \ll 1$ for (3.1) to hold. To estimate x from experiments, variations of θ/δ and C_f with R_δ are required. Here, θ is the momentum thickness, $C_f = 2(u_\tau/u_\infty)^2$ is the skin-friction coefficient and $R_\delta = \delta u_\infty/\nu$ is the Reynolds number based on δ and u_∞. Figure 3(*a*) shows that each of θ/δ and C_f follows two distinct power-law curve fits corresponding to two different regimes that cover the entire range of Reynolds numbers; these regimes will

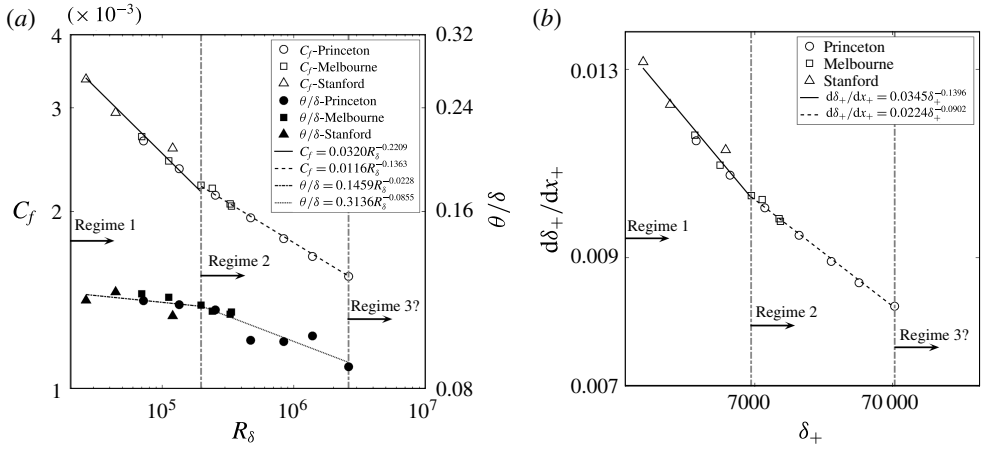

FIGURE 3. (*a*) Variation of C_f and θ/δ with Reynolds number R_δ and (*b*) variation of $\mathrm{d}\delta_+/\mathrm{d}x_+$ with Reynolds number δ_+ for the experimental ZPG TBL data of table 1. The lines indicate least-squares power-law curve fits to the data. The vertical dashed–dotted lines indicate demarcations between different regimes discussed in detail in § 3.

be discussed in some detail shortly. Substitution of the equations of these curve fits (depending on the regime) into the momentum integral equation $C_f/2 = \mathrm{d}\theta/\mathrm{d}x$ for ZPG TBLs (White 1994) and integration with the condition $\delta = 0$ at $x = 0$ (virtual origin) yield the expressions $x/\delta = 7.4375(S\delta_+)^{0.1981}$ and $x/\delta = 47.0556(S\delta_+)^{0.0508}$ for regimes 1 and 2 respectively (figure 3); the values of x in table 1 are computed using these expressions. Further, $\mathrm{d}u_\tau/\mathrm{d}x$ may be computed using $\mathrm{d}u_\tau/\mathrm{d}x = -(u_\infty/\delta S^2)\delta(\mathrm{d}S/\mathrm{d}x)$, wherein $\delta(\mathrm{d}S/\mathrm{d}x)$ may be estimated using (3.27) from Jones *et al.* (2008),

$$\delta\frac{\mathrm{d}S}{\mathrm{d}x} = \frac{S}{\kappa C_1 S^2 - \kappa C_2 S + C_2}. \tag{3.4}$$

It should be noted that C_1 and C_2 in (3.4) are integrals of $(u_\infty - \langle u\rangle)/u_\tau$ and $(u_\infty - \langle u\rangle)^2/u_\tau^2$ from $\eta = 0$ to $\eta = 1$ and are universal constants for defect profile similarity. Indeed, for all of the data of table 1, C_1 and C_2 are found to be fairly constant to within $\pm 7\,\%$ and $\pm 10\,\%$ of the respective average values of 4.118 and 27.555. Table 1 shows that all flows meet the condition $x/u_\tau(\mathrm{d}u_\tau/\mathrm{d}x) \ll 1$ quite well, i.e. (3.1) is valid.

Next, $\mathrm{d}\delta_+/\mathrm{d}x_+$ is computed using (3.3) and (3.4) with $\kappa = 0.4$ and is plotted in figure 3(*b*) against δ_+. Again, two distinct power-law curve fits characterize the regimes,

$$\frac{\mathrm{d}\delta_+}{\mathrm{d}x_+} = 0.0345\delta_+^{-0.1396}, \quad 1000 \leqslant \delta_+ < 7000, \tag{3.5}$$

$$= 0.0224\delta_+^{-0.0902}, \quad 7000 \leqslant \delta_+ < 70\,000, \tag{3.6}$$

with an unmistakable switchover around $\delta_+ = 7000$, which corresponds very well with the onset of a discernible log scaling region for even moments; see figures 4(*a*) and 11(*a,c,e*) from Vallikivi *et al.* (2015) and figures 1 and 3 from Meneveau & Marusic (2013). The regimes of figure 3(*a,b*) are identical and indicate consistent behaviour of data. The first regime, characterized by (3.5), begins around $\delta_+ = 1000$, where a discernible extent of mean velocity log scaling becomes apparent and continues to

grow with the Reynolds number. Variances, higher-order moments and the Reynolds shear stress do not exhibit log scaling in this regime. This regime is characterized by a set of power-law curve fits that describe variations of C_f, θ/δ and $\mathrm{d}\delta_+/\mathrm{d}x_+$, with Reynolds number δ_+ (figure 3). Around $\delta_+ = 7000$, discernible extents of log scaling of even moments and the Reynolds shear stress become apparent, in addition to the mean velocity, marking the onset of the second regime. Consistent with this, the power-law curve fits of C_f, θ/δ and $\mathrm{d}\delta_+/\mathrm{d}x_+$ also show a switchover, as seen in figure 3. Finally, the third regime begins around $\delta_+ = 70\,000$, beyond which odd-order moments also start to follow log scaling in addition to already established log variations of other quantities. The evidence towards the occurrence of the third regime is very limited (see the question marks in figure 3) since the present upper limit of the Reynolds number in laboratory experiments is close to $\delta_+ = 70\,000$ and therefore only one dataset (VHS7 from table 1 and figure 1*b*) shows the emergence of the log scaling of the third-order moment. Therefore, further high-*Re* TBL experiments are required to confirm and quantify the asymptotic log scaling of all moments in extreme-Reynolds-number situations.

In regimes 1 and 2 of figure 3(*b*), $\mathrm{d}\delta_+/\mathrm{d}x_+$ decreases with δ_+, indicating that $\mathrm{d}\delta_+/\mathrm{d}x_+ \to 0$ as $\delta_+ \to \infty$, which in turn leads to $\mathrm{ADV}_+(Q_+) \to 0$.

4. Conclusion

We have shown that zero advection, i.e. invariance along a mean-flow streamline, of a scaled mean quantity (dimensionless mean velocity or a generalized mixed moment) leads to log variation of that quantity in the ISL of a TBL flow. Conversely, the log variation of such a quantity leads to the corresponding zero-advection condition in the ISL. This is a generalization of a seminal result propounded by Coles (1955) for log scaling of the mean velocity. An equivalent kinematic description of this streamwise self-similarity is that the mean-flow streamlines essentially become straight and concurrent, emanating from a virtual wall source located a very large distance upstream of the measurement location, so that the condition $\mathrm{d}\delta_+/\mathrm{d}x \to 0$ is satisfied. This is further equivalent to the condition of the ratio of the mean velocities in the y and x directions remaining constant along a mean-flow streamline in the ISL; the iso-y_+ lines coincide with the mean streamlines in the inner layer, effectively sheltering it from the outer wake influence, and, from this, streamwise self-similarity in the ISL ensues.

It should be noted that the advection (on the left-hand side) in the dimensional/non-dimensional governing equation for Q is $\mathrm{ADV}(Q)$ or $\mathrm{ADV}_+(Q_+)$. If $Q_+ = Q/u_\tau^p$, then these advection terms are related to the present $\mathrm{ADV}(Q_+)$ as $\mathrm{ADV}(Q_+) = u_\tau^{-p}[\mathrm{ADV}(Q) + (p/x_s)]$ and $\mathrm{ADV}(Q_+) = u_\tau^2/\nu[\mathrm{ADV}_+(Q_+) - u_+(x/x_s)\partial Q_+/\partial x_+]$. It is therefore clear that $\mathrm{ADV}(Q_+) = 0$, i.e. invariance of the scaled mean quantity Q_+ along a mean streamline is not the same as $\mathrm{ADV}(Q) = 0$ or $\mathrm{ADV}_+(Q_+) = 0$ for the near-wall region, as used in Townsend (1976), George & Castillo (1997) and Wosnik, Castillo & George (2000). In fact, in developing flows such as TBLs, these two approaches coincide only when $x_s \to \infty$ as $\delta_+ \to \infty$.

For the mean velocity in ZPG TBLs, the two-way relation between the zero-advection condition and log scaling is satisfied in the ISL for arbitrary values of the Reynolds number, and therefore log scaling of the mean velocity occurs even at moderate Reynolds numbers that are capable of providing sufficient scale separation. For higher-order moments, the zero-advection condition is satisfied only at high Reynolds numbers when $\mathrm{d}\delta_+/\mathrm{d}x \to 0$, and this is consistent with the observation of

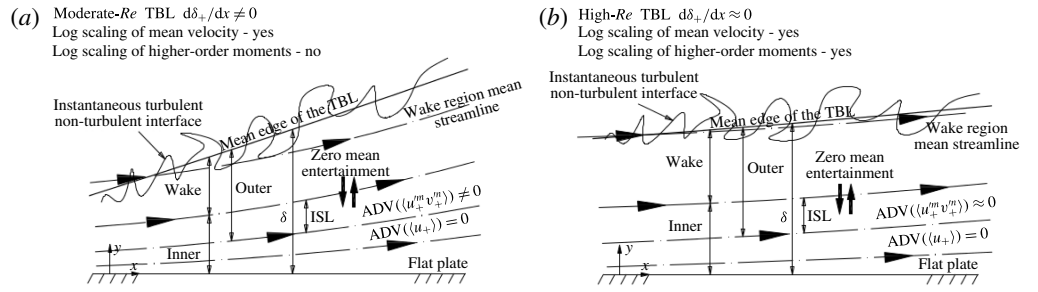

FIGURE 4. Pictorial representation of the conditions for log scaling emerging from the present work for canonical ZPG TBL flows at (*a*) moderate and (*b*) high Reynolds numbers. The dashed–dotted lines represent mean-flow streamlines, and in the inner region these are identical to the iso-y_+ lines. One should notice the difference in the inclination of a wake-region mean streamline in relation to the mean edge of the TBL in the two cases. The mean streamlines in (*b*), at high Reynolds numbers, tend to be straight and concurrent as if emanating from a virtual wall source at an infinite distance upstream.

log scaling of higher moments only at high Reynolds numbers (Marusic *et al.* 2013; Vallikivi *et al.* 2015). Figure 4 summarizes pictorially the main results of the present work.

In fully developed pipe and channel flows, (2.1) becomes degenerate, with each term becoming zero individually. Equivalently, (2.11) becomes singular, and the kinematic picture arising therefrom possibly consists of multiple virtual sources, at various heights from the wall, located an infinite distance upstream. Hence, the difference between TBLs and fully developed pipe/channel flows is subtle and needs further study.

It is known that odd moments of velocity fluctuations are strongly influenced by large-scale effects compared with even moments (Sreenivasan, Dhruva & Gil 1999; Mathis *et al.* 2011); δ_+ is a measure of the strength of these large-scale effects. In our analysis, the factor $\partial Q_+/\partial\delta_+$ in (2.6) represents sensitivity of the moment under consideration to variation of δ_+. Therefore, at a given value of δ_+, the magnitude of $\partial Q_+/\partial\delta_+$ may be expected to be smaller for an even moment compared with that for an odd moment. This is perhaps why, compared with even moments, a much smaller value of $d\delta_+/dx$ (and a much higher value of δ_+) is required in the case of odd moments to satisfy the zero-advection condition and make their log scaling evident. Experimental data from the literature suggest three broad Reynolds number regimes: $1000 \leqslant \delta_+ < 7000$, log scaling of the mean velocity; $7000 \leqslant \delta_+ < 70\,000$, log scaling of even moments and the Reynolds shear stress in addition to the mean velocity; $\delta_+ \geqslant 70\,000$, log scaling of odd moments as well (see § 3).

To conclude, it has been shown that streamwise self-similarity of a mean-flow quantity is a fundamental condition to be satisfied for the occurrence of log scaling of that quantity in the ISL of a TBL flow. For ZPG TBLs, apart from providing a large enough scale separation, increase of the flow Reynolds number is a means to satisfy (for different moments) the streamwise self-similarity condition to a progressively greater degree.

Acknowledgement

We sincerely thank Professor R. Narasimha for pointing out the connection between the present work and that of Coles (1955), and Professor I. Marusic for providing

the original Melbourne ZPG TBL data used in figure 1(*a*) and § 3. S.A.D. thanks the Director, Indian Institute of Tropical Meteorology (IITM), Pune for support.

References

COLES, D. E. 1955 The law of the wall in turbulent shear flow. In *50 Jahre Grenzschichtforschung*, pp. 153–163. F. Vieweg Braunschweig.

COLES, D. E. 1956 The law of the wake in the turbulent boundary layer. *J. Fluid Mech.* **1**, 191–226.

DEGRAAFF, D. B. & EATON, J. K. 2000 Reynolds-number scaling of the flat-plate turbulent boundary layer. *J. Fluid Mech.* **422**, 319–346.

FERNHOLZ, H. H. & FINLEY, P. J. 1996 The incompressible zero-pressure-gradient turbulent boundary layer: an assessment of the data. *Prog. Aerosp. Sci.* **32**, 245–311.

GEORGE, W. K. & CASTILLO, L. 1997 Zero-pressure-gradient turbulent boundary layer. *Appl. Mech. Rev.* **50** (12, part 1), 689–729.

HARUN, Z., MONTY, J. P., MATHIS, R. & MARUSIC, I. 2013 Pressure gradient effects on the large-scale structure of turbulent boundary layers. *J. Fluid Mech.* **715**, 477–498.

JONES, M. B., MARUSIC, I. & PERRY, A. E. 2001 Evolution and structure of sink-flow turbulent boundary layers. *J. Fluid Mech.* **428**, 1–27.

JONES, M. B., NICKELS, T. B. & MARUSIC, I. 2008 On the asymptotic similarity of the zero-pressure-gradient turbulent boundary layer. *J. Fluid Mech.* **616**, 195–203.

MARUSIC, I., CHAUHAN, K., KULANDAIVELU, V. & HUTCHINS, N. 2015 Evolution of zero-pressure-gradient boundary layers from different tripping conditions. *J. Fluid Mech.* **783**, 379–411.

MARUSIC, I., MATHIS, R. & HUTCHINS, N. 2010*a* Predictive model for wall-bounded turbulent flow. *Science* **329**, 193–196.

MARUSIC, I., MCKEON, B. J., MONKEWITZ, P. A., NAGIB, H. M., SMITS, A. J. & SREENIVASAN, K. R. 2010*b* Wall-bounded turbulent flows at high Reynolds numbers: recent advances and key issues. *Phy. Fluids* **22** (6), 065103.

MARUSIC, I., MONTY, J. P., HULTMARK, M. & SMITS, A. J. 2013 On the logarithmic region in wall turbulence. *J. Fluid Mech.* **716**, R3.

MATHIS, R., MARUSIC, I., HUTCHINS, N. & SREENIVASAN, K. R. 2011 The relationship between the velocity skewness and the amplitude modulation of the small scale by the large scale in turbulent boundary layers. *Phys. Fluids* **23**, 121702.

MENEVEAU, C. & MARUSIC, I. 2013 Generalized logarithmic law for high-order moments in turbulent boundary layers. *J. Fluid Mech.* **719**, R1.

MONKEWITZ, P. A., CHAUHAN, K. A. & NAGIB, H. M. 2008 Comparison of mean flow similarity laws in zero pressure gradient turbulent boundary layers. *Phys. Fluids* **20**, 105102.

MONKEWITZ, P. A. & NAGIB, H. M. 2015 Large-Reynolds-number asymptotics of the streamwise normal stress in zero-pressure-gradient turbulent boundary layers. *J. Fluid Mech.* **783**, 474–503.

SREENIVASAN, K. R., DHRUVA, B. & GIL, I. S. 1999 The effects of large scales on the inertial range in high-Reynolds-number turbulence. arXiv:chao-dyn/9906041.

TALLURU, K. M., BAIDYA, R., HUTCHINS, N. & MARUSIC, I. 2014 Amplitude modulation of all three velocity components in turbulent boundary layers. *J. Fluid Mech.* **746**, R1.

TENNEKES, H. & LUMLEY, J. L. 1972 *A First Course in Turbulence*. MIT Press.

TOWNSEND, A. A. 1976 *The Structure of Turbulent Shear Flow*, 2nd edn. Cambridge University Press.

VALLIKIVI, M., HULTMARK, M. & SMITS, A. J. 2015 Turbulent boundary layer statistics at very high Reynolds number. *J. Fluid Mech.* **779**, 371–389.

VAN DYKE, M. 1975 *Perturbation Methods in Fluid Mechanics*. Parabolic Press.

WHITE, F. M. 1994 *Fluid Mechanics*, 4th edn. McGraw-Hill, International Edition.

WOSNIK, M., CASTILLO, L. & GEORGE, W. K. 2000 A theory for turbulent pipe and channel flows. *J. Fluid Mech.* **421**, 115–145.